Geophys. J. Int. (2009) **177,** 913–924 doi: 10.1111/j.1365-246X.2008.04082.x

Palaeclimatic significance of the Xiantai fluvio-lacustrine sequence in the Nihewan Basin (North China), based on rock magnetic properties and clay mineralogy

Hong Ao,[1,2] Mark J. Dekkers,[3] Chenglong Deng[1] and Rixiang Zhu[1]

[1]*Paleomagnetism and Geochronology Laboratory (SKL-LE), Institute of Geology and Geophysics, Chinese Academy of Sciences, Beijing* 100029*, China. E-mail: ah@mail.iggcas.ac.in*

[2]*Graduate University of Chinese Academy of Sciences, Beijing* 100049*, China*

[3]*Paleomagnetic Laboratory 'Fort Hoofddijk', Department of Earth Sciences, Faculty of Geosciences, Utrecht University, Budapestlaan* 17, 3584 *CD Utrecht, The Netherlands*

Accepted 2008 November 28. Received 2008 November 28; in original form 2008 August 13

SUMMARY

Here, we report an increased cooling coupled with an intensified aridification for the Xiantai fluvio-lacustrine sequence of Pleistocene age (1.9–0.1 Ma) in the Nihewan Basin (North China), known for the occurrence of several hominin sites. The cooling is related to an up-section decrease in propensity to chemical weathering as inferred from an increase in low-field susceptibility after cycling to 700 °C. Close to 700 °C, reacting chlorite is providing the iron source for newly formed very fine-grained ferrimagnetic minerals which enhances the susceptibility signal. The reactivity of chlorite after annealing at temperatures above 600 °C is documented with X-ray diffraction and the up-section decrease in propensity to chemical weathering is confirmed by the up-section declining illite/chlorite ratios and increasing chlorite and illite contents based on X-ray diffraction analysis on selected samples.

Key words: Environmental magnetism; Magnetic mineralogy and petrology; Rock and mineral magnetism; Asia.

1 INTRODUCTION

The recent years have witnessed a considerable progress in the palaemagnetic dating of the stratigraphy in the Nihewan Basin (North China), which is famous for its well-developed late Cenozoic strata that are rich in Palaelithic sites and mammalian faunas of the early Pleistocene (Teilhard de Chardin & Piveteau 1930; Qiu 2000; Zhu *et al.* 2003, 2007; Deng *et al.* 2008). The mammalian fossils contained in this sedimentary sequence, known as the Nihewan faunas, traditionally correspond to the Villafranchian fauna in Europe (Teilhard de Chardin & Piveteau 1930; Qiu 2000). The improved age frame led to a better understanding of a series of important issues, such as early human occupation in the Old World, the infilling history of the Nihewan Basin, and the chronological sequence of the Nihewan faunas (Løvlie *et al.* 2001; Zhu *et al.* 2001, 2003, 2004, 2007; Wang *et al.* 2004, 2005, 2008; Deng *et al.* 2006a, 2007, 2008; Li *et al*. 2008).

Most hominin or Palaelithic sites in China from the early Pleistocene are found in the Nihewan Basin (around 40°N). These include the sites of Majuangou (1.55 − 1.66 Ma) (Zhu *et al.* 2004), Xiaochangliang (1.36 Ma) (Zhu *et al.* 2001), Xiantai (1.36 Ma) (Deng *et al.* 2006a), Banshan (1.32 Ma) (Zhu *et al.* 2004), Feiliang (1.2 Ma) (Deng *et al.* 2007), Donggutuo (1.1 Ma) (Wang *et al.* 2005), Cenjiawan (1.1 Ma) (Wang *et al.* 2006) and Maliang (0.78 Ma) (Wang *et al.* 2005). As a result, the plethora of early Pleistocene Palaelithic sites in the basin provides an excellent opportunity to explore early human adaptability to high northern latitude (around 40°N) East Asia (Zhu *et al.* 2001, 2004; Deng *et al.* 2006a, 2007). However, little is known about the long-term palaeclimatic records retrieved from the Nihewan sedimentary sequences bearing these Palaelithic sites.

Magnetic parameters are often determined rather quickly and can be evaluated from almost all rocks. Environmental Magnetism utilizes variations in a set of magnetic properties to reconstruct palaeenvironmental conditions (Verosub & Roberts 1995; Evans & Heller 2003). Like magnetic minerals clay minerals such as chlorite and illite may contain relevant palaeenvironmental information (Righi *et al.* 1995; Kalm *et al.* 1996). In recent years, magnetic and clay minerals have been successfully employed to trace the palaeenvironmental variations recorded in the Chinese loess-palaesol sequences and in marine sediments (Heller & Evans 1995; Verosub & Roberts 1995; Kalm *et al.* 1996; Sagnotti *et al.* 1998; Deng *et al.* 2005, 2006b; Wan *et al.* 2006, 2007; Liu *et al.* 2007). However, the palaeenvironmental significance of these minerals in the Nihewan fluvio-lacustrine sediments has not been systematically investigated yet.

In this study, we present a detailed rock magnetic and clay mineralogical investigation on the Xiantai fluvio-lacustrine sequence in the Nihewan Basin, which contains the Xiantai (also named Dachangliang) stone artefact layer (Pei 2002; Deng *et al.* 2006a). Based on the rock magnetic properties and clay mineralogy of the sediments, we generate a series of independent proxies for

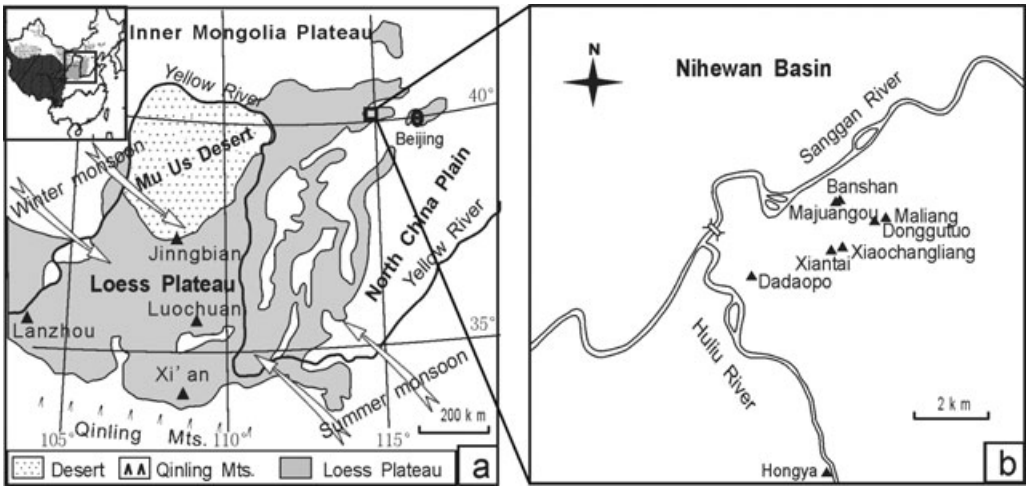

Figure 1. Schematic map of the Nihewan Basin and the Xiantai section (modified from Deng *et al.* 2006a). The Yellow River and Yangtze River are the major river systems in north and south China, respectively. The east–west trending Qinling Mountains are the traditional dividing line between temperate northern China and subtropical southern China. The arrows show the summer or winter monsoon directions.

Pleistocene palaeclimatic changes in this basin. Comparing our results with data from this basin and the Chinese Loess Plateau, we aim to reconstruct the Pleistocene environmental evolution in this area.

2 GEOLOGICAL SETTING AND SAMPLING

The Nihewan Basin is an inland basin between the North China Plain and the Inner Mongolian Plateau (Fig. 1a). Extensive sedimentary exposures consisting of well-developed fluvio-lacustrine sediments of late Cenozoic age are found along the SW–NE trending Sanggan River (Fig. 1b). This fluvio-lacustrine sequence in the basin is capped by the Holocene soil (S0) and/or the last glacial loess (L1) and/or the last interglacial soil (S1) (Deng *et al.* 2008). It is underlain by Pliocene red clay of aeolian origin or by Jurassic breccia.

The Xiantai [also named Dachangliang (Pei 2002) section (40°13.126′N, 114°39.623′E) lies at the eastern margin of the Nihewan Basin (Fig. 1b). Here, the fluvio-lacustrine sequence has a thickness of 64.5 m, which is mainly composed of greyish-white clays, greyish-green clayey silts and greyish-yellow silts and is intermediated by some fine-grained sands. It is capped by the aeolian S0 (0.4 m), L1 (5.75 m) and S1 (2.3 m) and underlain by Jurassic breccia. Magnetostratigraphic results show that the Xiantai fluvio-lacustrine sequence is of a lower Olduvai to late Brunhes age (Deng *et al.* 2006a). Integrated magnetostratigraphic, lithostratigraphic and magnetic susceptibility correlation between the Xiantai and Xiaochangliang sections date the Xiantai artefact layer at ca. 1.36 Ma (Deng *et al.* 2006a). An age-depth model for the Xiantai section is established through linear interpolation of six palaemagnetically controlled ages (Deng *et al.* 2006a; Fig. 2a). Due to the lack of other constrained ages in the top of Xiantai fluvio-lacustrine sequence, here we use the bottom age of S1 (0.13 Ma) (Ding *et al.* 2002) as the ending age of this sequence. The deposition of this sequence commenced approximately from the lower Olduvai subchron (Deng *et al.* 2006a), which has been dated to span from 1.95 to 1.77 Ma (Berggren *et al.* 1995), thus 1.9 Ma is used to control the bottom age.

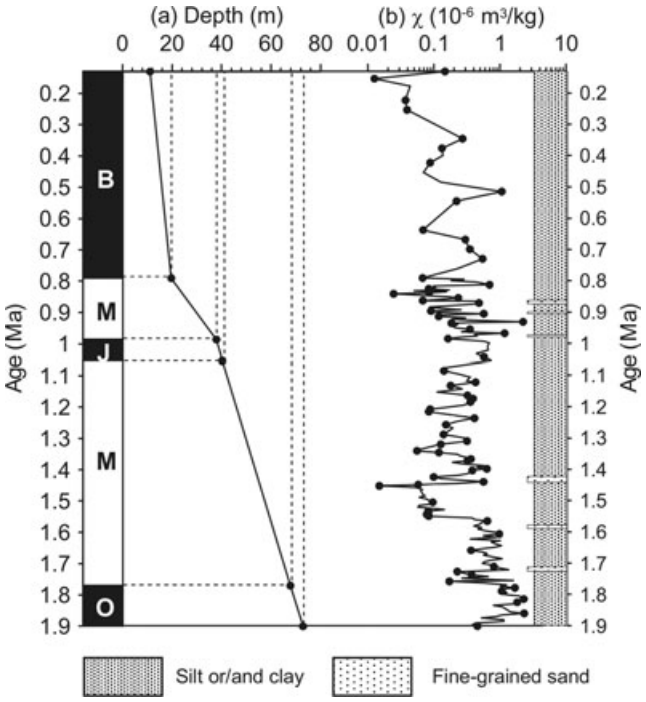

Figure 2. (a) Age-depth models and geomagnetic polarity timescale (GPTS; Berggren *et al.* 1995; Singer *et al.* 1999, 2002). (b) Lithostratigraphy and χ profile. The lithostratigraphy and polarity data were from Deng *et al.* (2006a). The solid circles in (b) represent the samples selected for this study. B, Brunhes; J, Jaramillo; M, Matuyama; O, Olduvai.

Our previous magnetostratigraphic study of the Xiantai section (Deng *et al.* 2006a) was based on 196 oriented block samples from the depth interval of 11–73 m (0.13–1.9 Ma) with a spacing of 20–40 cm. Here, we use the unheated left-overs of that collection. For the present mineral magnetic and clay mineralogical investigation, 72 representative samples were selected from different stratigraphic intervals characterized by maxima and minima in magnetic susceptibility (Fig. 2b).

3 METHODS

Low-field magnetic susceptibility (χ, calculated on a mass-specific basis) was measured with a Bartington MS2 meter at a frequency of 470 Hz. In addition, high-frequency magnetic susceptibility was measured at a frequency of 4700 Hz to calculate the frequency-dependent susceptibility χ_{fd} per cent [χ_{fd} per cent = $(\chi_{470\,Hz}-\chi_{4700\,Hz})/\chi_{470\,Hz} \times 100$ per cent]. The noise during measurement was $<0.1 \times 10^{-8}$ m^3/kg and susceptibilities of our samples ranged between 1×10^{-8} m^3/kg and 232×10^{-8} m^3/kg. Temperature-dependent susceptibility measurements ($\chi-T$ curves) were obtained by cycling samples in an argon atmosphere (the flow rate is 100 ml/min) at a frequency of 875 Hz from room temperature up to 300–700°C and back to room temperature using a KLY-3 susceptibility bridge equipped with a CS-3 high-temperature furnace (sensitivity of 1×10^{-8} SI, AGICO Ltd., Brno, Czech Republic). Each cycle started with powdered samples of ∼300 mg with a heating and cooling rate of 11°C/min. The magnetic field during measurement was 300 A/m. The noise was $<0.2 \times 10^{-8}$ m^3/kg and all the $\chi-T$ curves were corrected for noise. We defined an alteration index AH-ratio, to quantitatively characterize the change in magnetic susceptibility after heating to 700°C:

$$AH-\text{ratio} = (\chi_{post}-\chi_{pre})/\chi_p \times 100\,\text{per cent}. \quad (1)$$

Here, χ_{pre} and χ_{post} were the magnetic susceptibilities before and after heating to 700 °C, respectively. χ_p was the paramagnetic susceptibility calculated from the slope at high fields (between 800 and 1000 mT) of the hysteresis loops. A positive alteration index value indicated a higher susceptibility during cooling than heating, while a negative index indicated the opposite relationship.

Anhysteretic remanent magnetization (ARM) of the heated samples was acquired in a 100 mT AF and a 0.05 mT constant biasing field, and was measured with a 2G Enterprises Model 760-R cryogenic magnetometer with a sensitivity of 0.2×10^{-11} A m^2 housed in a magnetically shielded room with a residual field below 300 nT. The noise was 1.6×10^{-9} A m^2.

Room temperature hysteresis loops and first-order reversal curve (FORC) diagrams were measured using a MicroMag 2900 alternating gradient magnetometer (Princeton Measurements Corp., USA) on 72 and 20 samples, respectively. A piece or a powdered raw sample of ∼10 mg was measured with a step of 2 mT up to 1 or 1.5 T. Following Roberts *et al*. (2000), 125 FORCs were measured for each sample. All these hysteresis measurements were obtained with the following instrument parameters: probe factor of 5×10^5 V A^{-2}, sensitivity of 1×10^{-11} A m^2, averaging time of 100 or 200 ms. The mean noise was about 6.5×10^{-11} A m^2 with a standard deviation of about 5.6×10^{-11} A m^2. The magnetic moment of most samples was $>1.0 \times 10^{-8}$ A m^2.

Low-temperature magnetic measurements of both unheated and heated samples were performed on a Quantum Design superconducting quantum interference device (SQUID) Magnetic Properties Measurement System (MPMS). Zero-field warming of the isothermal remanent magnetization acquired in 5 T at 5 K (hereafter termed 5T-IRM@5K) was measured at a temperature increment of 5 K from 5 to 300 K. Low-temperature dependence of susceptibilities at frequencies of 1.4, 140, 400, 1000 and 1400 Hz respectively, was also measured between 5 and 300 K with a temperature increment of 5 K.

X-ray diffraction (XRD) analyses (scanning from 3° to 65° or 70° 2θ) of the unheated and heated samples were carried out using a DMAX2400 X-ray diffractometer with the following parameters: Cu-Kα/40kV/40mA, divergence slit of 1°, scattering slit of 1°, receiving slit of 0.3 mm, continuous scan mode, scanning speed of 4° min^{-1} and scanning step of 0.02°. Following Wan *et al.* (2006, 2007), the heights of reflection of chlorite at 7 Å and illite at 10 Å were used to semi-quantitatively estimate their relative content in the sediments, respectively.

4 RESULTS

4.1 $\chi-T$ curves

All samples showed a major drop in χ at ∼580 °C(Figs 3a–e, k and l) except for sample DCL004 (inferred age 222.1 ka), suggesting the presence of magnetite. Some samples had a faint drop of χ between ∼300 and ∼400 °C (Figs. 3c–e and j), which might arise from the conversion of metastable maghemite to weakly magnetic hematite (Oches & Banerjee 1996; Florindo *et al.* 1999; Liu *et al.* 2005). Hematite was usually not obvious in the $\chi-T$ curves due to its weak magnetism, however, some $\chi-T$ curves still displayed a decreased χ between ∼580 and ∼680°C (Figs 3a-c), suggesting a relatively high concentration of hematite in these samples. Hematite was the dominant characteristic remanence carrier in these samples as suggested by progressive demagnetisation of the natural remanent magnetization (e.g. Deng *et al.* 2006a).

The incremental heating $\chi-T$ curves of sample DCL004 and DCL019 (inferred age 697.9 ka) were also shown here (Figs 3f–l). The heating and cooling curves were almost reversible for heating up to 300, 400 and 500 °C, suggesting that no obvious magneto mineralogical changes was induced by the heating. There was a slightly increased cooling after heating to 600 °C. After heating to 700 °C, however, most samples showed an increased cooling along with an increased χ at ∼580 °C and a distinct kink between ∼400 and ∼500 °C, suggesting the significant neoformation of magnetite and possible thermally stable maghemite (De Boer & Dekkers 2001) during thermal treatment between 600 and 700 °C.

4.2 Low-temperature magnetic measurements

Susceptibility variations between 5 and 300 K of the unheated samples were independent of frequency (Fig. 4a), indicating that superparamagnetic (SP) particles were not prominent in the natural samples, which was consistent with the low values of room-temperature χ_{fd} per cent (usually between l and 5 per cent). Thus, the sharp decrease of the χ (Fig. 4a) and 5T-IRM@5K (Fig. 4b) upon warming from 5 to 50 K might be mainly caused by the paramagnetic minerals that ordered at very low temperature and therefore unblocked when warming through this temperature range (Coey 1988). This interpretation agreed with the high values of the high-field slope of the hysteresis loops (Ao *et al.* 2007). In line with the χ–T curves (Fig. 3), magnetite was evidenced by remanence loss at the Verwey transition (Fig. 4b). This transition was much more pronounced in the dM/dT curve. For the heated samples, the magnetic susceptibility gradually decreased with increasing frequency and showed a broad maximum around ∼100 K (Fig. 4c), suggesting that the grain size of newly formed ferrimagnetic minerals during heating was very fine (i.e. SP), according with the significant increase in χ_{fd} per cent (>10 per cent). Furthermore, a significant decrease in χ of the unheated samples was replaced by a significant increase in χ of the heated samples when warming from 5 to 50 K, implying that the newly formed fine-grained ferrimagnetic minerals were possibly produced through annealing of paramagnetic minerals (e.g. chlorite). After heating, the Verwey transition became very subdued (Fig. 4d), which might be due to the significant production of

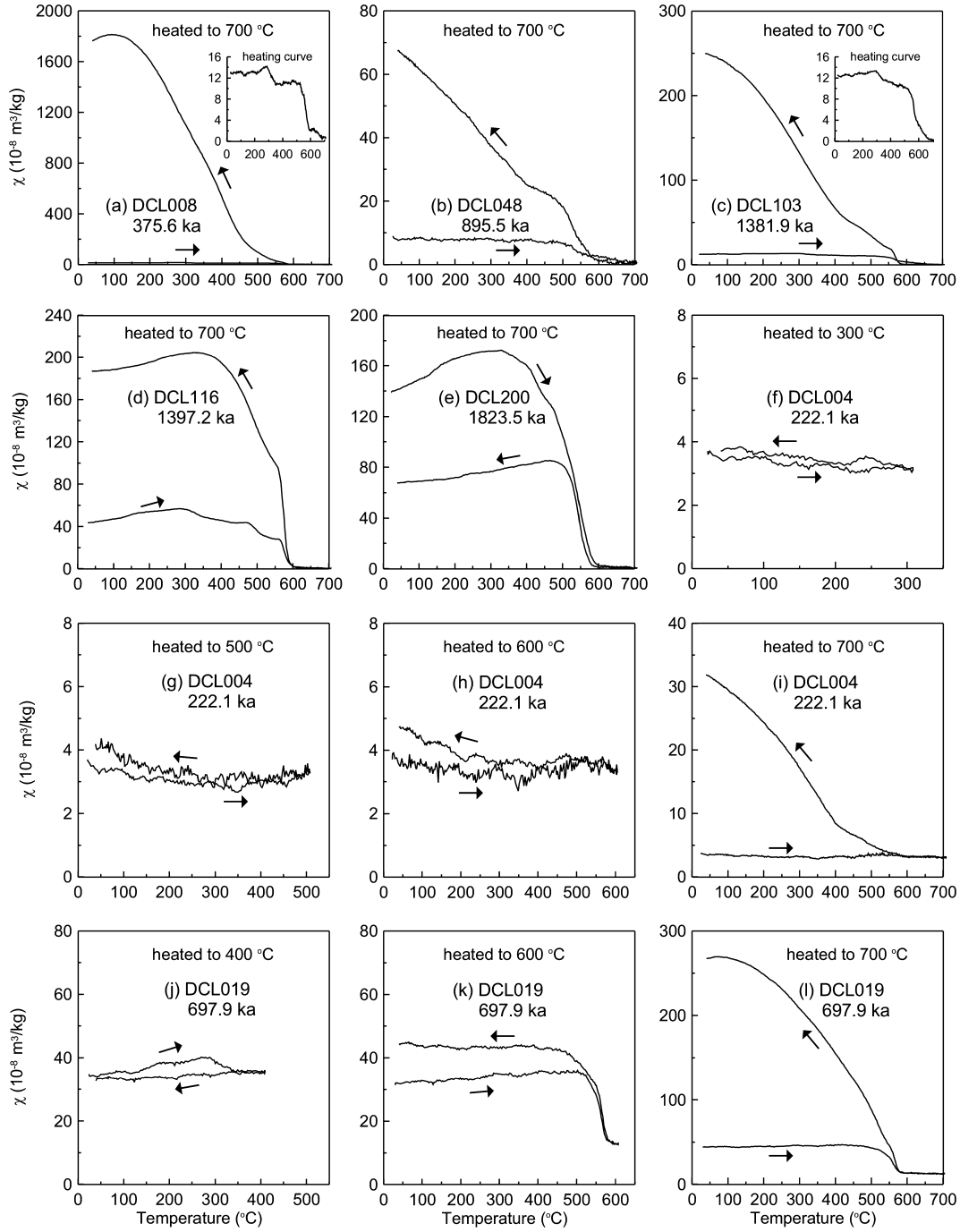

Figure 3. $\chi - T$ curves of typical samples from the Xiantai section. Samples in (a)–(e) are directly heated to 700 °C. (f)–(i) Sample DCL004 and (j)–(l) sample DCL019 are stepwise heated to 700 °C.

fine-grained (SP) ferrimagnetic minerals that did not show the Verwey transition. Compared to the unheated samples, the 5T-IRM@5K of the heated sample increased by more than a factor of 15 and showed a more rapid and significant decrease upon warming from 5 to 50 K, which was probably caused by SP particles that order at very low temperature and therefore unblock when warming through this temperature range (Dunlop & Özdemir 1997) and/or magnetic interaction and surface effects in very fine particles (Passier & Dekkers 2002) rather than the ordering and then unblocking of paramagnetic minerals because most of the paramagnetic minerals were suggested to be replaced by fine-grained ferrimagnetic minerals.

4.3 Hysteresis properties

The combined Day plot and FORC diagram served as a powerful tool of identifying the coercivity and grain size distribution of magnetic materials (Day *et al.* 1977; Roberts *et al.* 2000; Dunlop 2002a,b). It should be noted that both the presence of SP magnetic grains and hematite could increase the ratio of B_{cr} / B_c, which, in turn, led the hysteresis parameters to be shifted towards the right to some extent in the Day plot (Roberts *et al.* 1995; Dunlop & Özdemir 1997). Most of the unheated samples showed a pseudo-single-domain (PSD) magnetite character in the FORC diagrams

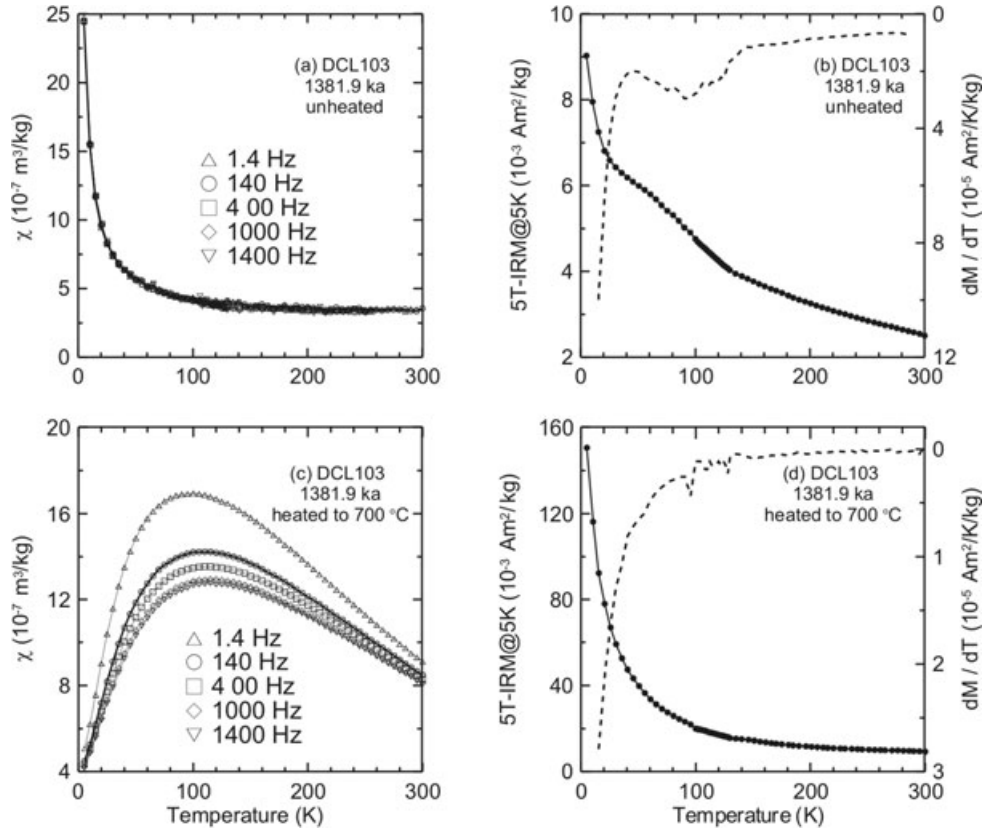

Figure 4. (a) and (c) frequency and temperature dependence of magnetic susceptibility of unheated and heated sample DCL103 at low temperature. (b) and (d) Thermal warming of low temperature 5T-IRM@5K (solid circles) and the first derivatives dM/dT (dashed line) for selected unheated and heated sample DCL103.

(Figs 5a and b) (Roberts *et al.* 2000) and mainly located between the single-domain (SD) + SP and SD + multidomain (MD) curves in the PSD range of the Day plot (Fig. 5c). A small number of unheated samples located in the SD + SP range or slightly shift over the right sideline of the PSD range in the Day plot (Fig. 5c), while the corresponding FORC diagrams did not show an SD or SP but PSD character (e.g. Fig. 5a). These properties seemed to be inconsistent, which was possibly caused by the decreased magnetite and increased hematite contents that led to the ambiguity in the Day plot. This interpretation coincided with the relatively noisier FORC diagrams (e.g. Fig. 5a) under the same smoothing factor and lower S^*-ratios of these samples (varying from 0.66 to 0.99, not shown). After heating, however, in addition to PSD magnetite particles, the closed inner contours in the FORC diagram also revealed the presence of SD magnetite particles (Fig. 5d) (Roberts *et al.* 2000). Furthermore, the contours in the left-hand corner of the FORC diagram showed the behaviour of SP magnetite particles as well (Fig. 5d) (Roberts *et al.* 2000; Pike *et al.* 2001). The shift of the hysteresis ratios of the heated samples in the Day plot (Fig. 5c) accorded with the properties as emerging from the FORC diagrams.

Most samples from the Xiantai section contained a significant paramagnetic contribution. After correction for the paramagnetic signal, the samples exhibited two types of hysteresis loops. One was characterized by a wasp-waisted behaviour with an open nature up to 500–900 mT (e.g., Figs 6a–c), suggesting the coexistence of two magnetic mineral components with strongly contrasting coercivities (Roberts *et al.* 1995). The two magnetic phases were low-coercivity magnetite and high-coercivity hematite, indicated from $\chi - T$ curves (Fig. 3) and the behaviour during progressive demagnetization of the natural remanent magnetization (Deng *et al.* 2006a), respectively. The other type of hysteresis loop was characterized by a closed nature below 200 mT (e.g., Fig. 6d), indicating the dominance of low-coercivity components. In addition, the heated samples exhibited more pronounced wasp-waisted hysteresis loops, along with a closed behaviour at much lower field (below 200 mT) (e.g., Figs 6e and f). The coercivity contrast with a low average coercivity range caused by the neoformation of SP and SD ferrimagnetic minerals during heating might significantly contribute to this soft-component-dominated wasp-waisted hysteresis loop (*cf*. Roberts *et al.* 1995).

4.4 XRD analyses

XRD analyses suggested that the clay minerals are dominantly chlorite and illite (Figs 7a, f, h and j). Besides these clay minerals, quartz and anorthite were important components in the samples as well (Fig. 7). Importantly, the XRD spectra did not suggest the presence of chlorite in the samples after 700 °C thermal treatment, indicative of its decomposition during laboratory heating. Furthermore, samples containing higher content of chlorite seemed to have higher increase in χ after heating. For example, sample DCL008 (inferred age 375.6 ka) (Fig. 7f) exhibited a stronger chlorite signal than the other samples (Figs 7a, h and j), in line with its higher increase in χ after heating to 700 °C (Fig. 3). Thus, the XRD spectra data provided evidence that the χ increases due to neoformation of

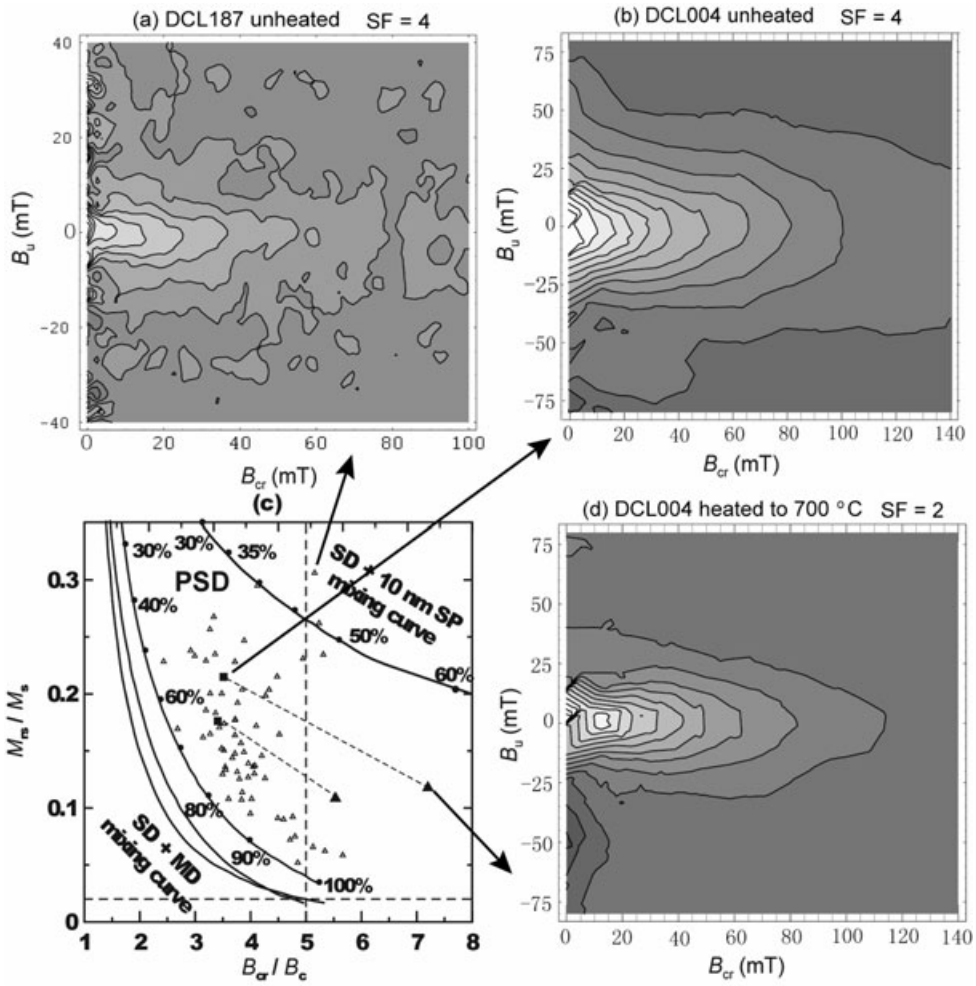

Figure 5. (a)–(b) and (d) FORC diagrams for representative samples, and the corresponding hysteresis ratios plotted on a Day plot (c) (Day *et al.* 1977; Dunlop 2002a). Solid triangles in (c) represent the heated samples. Open triangles and solid squares represent the unheated samples.

ferrimagnetic materials were mainly derived from the decomposition of chlorite at high temperature. In addition, the XRD spectra of the incrementally heated samples revealed that the decomposition of chlorite mainly occurred at temperatures higher than 600 °C (Figs 7a–e). Below 600 °C, the changes in the chlorite reflections were not significant (Figs 7a–c). After heating up to 600°C, however, the chlorite reflections reduced significantly in intensity (Fig. 7d). They disappeared entirely after heating up to 700 °C (Fig. 7e). These behaviours agreed with the incremental heating $\chi - T$ curves.

5 DISCUSSION

5.1 Magnetic and clay mineralogy of the Xiantai fluvio-lacustrine sequence

A ferrimagnetic mixture of magnetite, maghemite and hematite in the Xiantai fluvio-lacustrine sediments is suggested by our multiparameter rock magnetic investigation. The magnetic properties of the natural samples are dominated by PSD magnetite and fine-grained magnetic particles such as SD and SP grains are not prominent, judging from the combined Day and FORC diagrams (Fig. 5), frequency-independent χ at low temperature (Fig. 4a) and low values of χ_{fd} per cent at room temperature.

Magnetite in lake sediments originates from detrital input and/or authigenic or biogenic processes during deposition (Hu *et al.* 2002; Evans & Heller 2003). However, authigenic SD magnetite (magnetosomal SD particles) is not found in the Nihewan fluvio-lacustrine sediments, suggesting that authigenic and biogenic processes in the sedimentary sequence are not prominent. This is also supported by the extremely low ARM/SIRM ratios throughout this section (<0.03), the Donggutuo (<0.04) (Wang 2007) and the Xujiayao (Wang *et al.* 2008) sections because this ratio for the intact magnetosomal SD magnetite is usually between 0.15 and 0.25 (Moskowitz *et al.* 1993). In addition, neither the present nor the previous investigations on the Nihewan fluvio-lacustrine sediments have suggested the presence of greigite that are usually considered as authigenic origin (Roberts 1995; Rowan & Roberts 2006). Furthermore, authigenesis of magnetic minerals in lake sediments significantly depends on the aquatic productivity and nutrient availability (Hilton 1987). Thus, it is expected that the magnetite in the Nihewan fluvio-lacustrine sediments is mainly of detrital origin from the deposits in the catchment regolith (Deng *et al.* 2008; Wang *et al.* 2008), according with the PSD character of the magnetite grains suggested by our mineral magnetic measurements and previous studies (e.g.

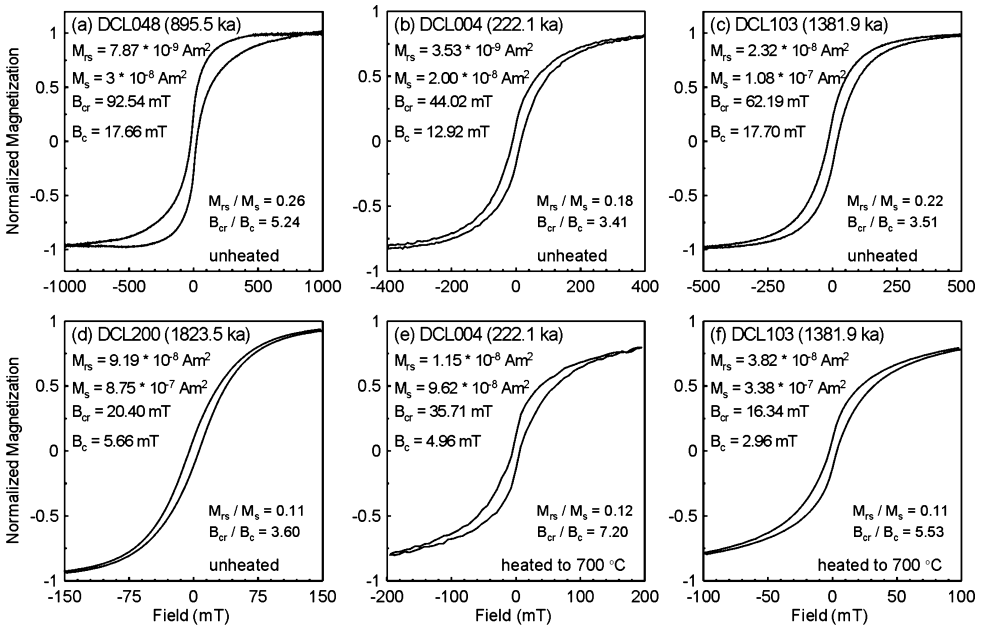

Figure 6. Hysteresis loops for representative unheated and heated samples after correction for paramagnetic contribution. The hysteresis loop of sample DCL004 was measured in fields up to ±1.5 and others in fields up to ±1.0 T.

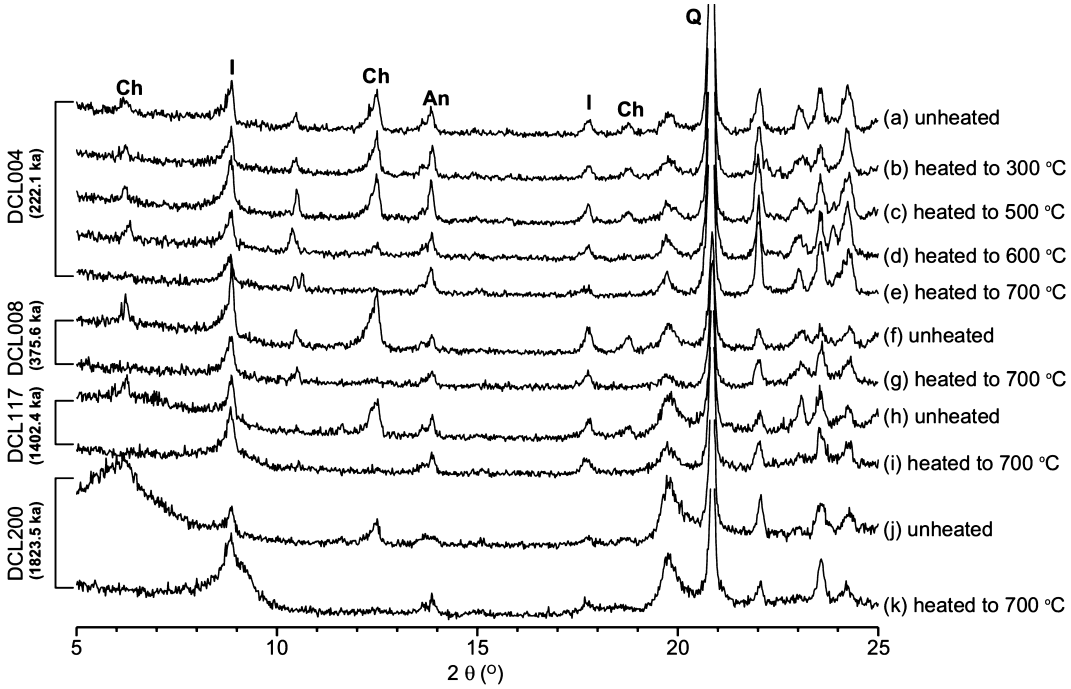

Figure 7. XRD spectra for representative unheated and heated samples. Numbers indicate the temperature of the thermal treatment. Ch, chlorite; I, illite; Q, quartz and An, anorthite.

Wang *et al.* 2002**;** Deng *et al.* 2006a**,** 2008; Ao *et al.* 2007; Wang 2007).

After heating up to 700 °C in an argon atmosphere, a large amount of SP and SD ferrimagnetic minerals was formed. This is evidenced by significant increase in χ after heating (Fig. 3), low-temperature magnetic measurements (Fig. 4), measurements of hysteresis parameters (Figs 5 and 6), and positive correlation of *AH*-ratio with χ (correlation coefficient of $R = 0.92$), χ_{fd} per cent (correlation coefficient of $R = 0.82$) (Figs 8a and b) and ARM (correlation coefficient of $R = 0.56$) of the heated samples (Fig. 8c). Both decomposition of iron-containing silicates (clay minerals) (Deng *et al.* 2005; Ao 2008) and desorption of sorbed iron-(oxy-hydr) oxides onto silicates (Hirt *et al.* 1993) can deliver the source of iron required for the neoformation of fine-grained ferrimagnetic minerals. However, the incrementally heating runs of selected samples show that χ does not increase significantly below the 600 °C treatment (e.g. Figs 3f–h, j and k), which indicates that the χ increase results mainly from decomposition of iron-containing silicates/clay minerals. From the XRD analyses, chlorite is suggested to be the main contributor to the neoformation of fine-grained ferrimagnetic minerals during

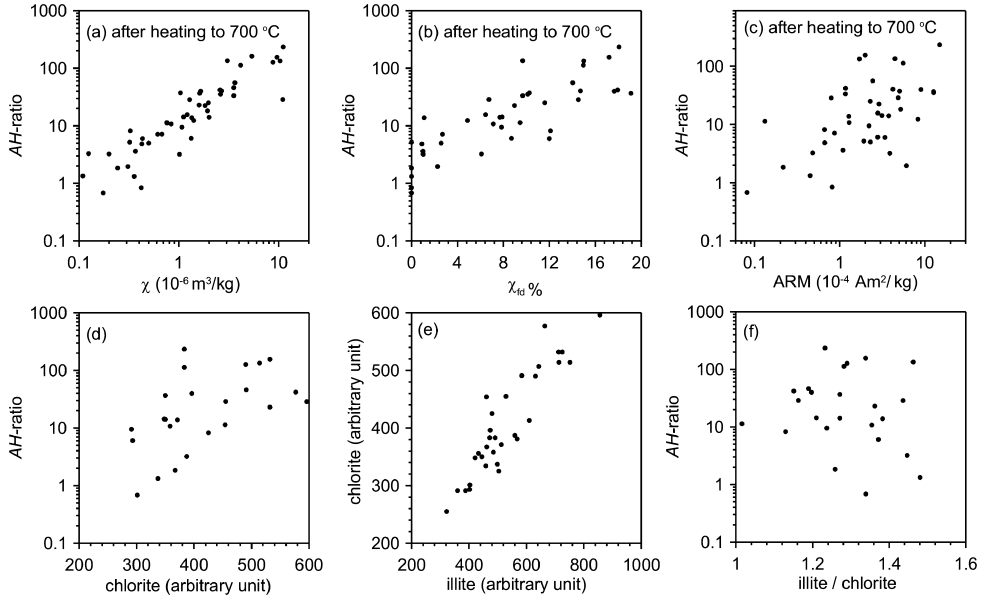

Figure 8. *AH*-ratio versus (a) χ, (b) χ_{fd} per cent and (c) ARM of the heated samples. (d) *AH*-ratio versus chlorite content in the unheated samples. (e) Chlorite content versus illite content in the unheated samples. (f) *AH*-ratio versus illite/chlorite ratios for the unheated samples.

heating, leading to increase in χ, even though some other magnetic and non-magnetic minerals might have contributed, perhaps small quantities, to this as well. Thus, the parameter *AH*-ratio characterizing the relative amount of newly formed fine-grained ferrimagnetic minerals during heating can be used to assess the relative concentration of chlorite in the samples, which is supported by the positive correlation between *AH*-ratio and chlorite content, with a correlation coefficient of $R = 0.55$ (Fig. 8d).

5.2 Weathering indices and palaeclimatic significance

Chlorite is a common iron-rich clay mineral in the loess, marine and lake sediments. The chlorite contained in the Nihewan fluvio-lacustrine sediments derives mainly from detrital material eroded from the catchment regolith, which is prone to be altered due to chemical weathering in natural environments (Proust *et al.* 1986; Righi *et al.* 1995). Chlorite weathering resulting in its transformation into illite-montmorillonite releases iron, which forms iron oxides (Proust *et al.* 1986; Righi *et al.* 1995). The positive correlation between the mica/chlorite ratio and susceptibility in the Luochuan Chinese loess section suggests that chlorite weathering is also relevant to the increase of susceptibility of palaesols (Ji *et al.* 1999). Thus, the chlorite content (or *AH*-ratio in this case) is shown to be negatively correlated to the degree of chemical weathering. For the Nihewan fluvio-lacustrine sediments, the detrital chlorite is hard to alter after deposition and its content is mainly related to chemical weathering in the catchment regolith before deposition. Therefore, the thermally induced rock magnetic signals of the chlorite in the Nihewan sediments may be used to retrieve the palaeclimatic conditions in this area. It is expected that the extent of *in situ* chemical weathering in this region is lower during cold/dry periods, and is higher during warm/humid periods. Higher (lower) *AH*-ratio would suggest higher (lower) content of chlorite, thus representing lower (higher) chemical weathering intensity and corresponding to cold/dry (warm/humid) climate.

The positive and linear correlation between illite and chlorite (Fig. 8e), with a correlation coefficient of $R = 0.91$, indicates that these two clay materials have a consistent pattern of cyclic change with climate and the provenance of the Nihewan fluvio-lacustrine sediments did not change significantly. Both illite and chlorite are prone to chemical weathering, however, chlorite is more susceptible to chemical weathering than illite, thus the illite/chlorite ratio has been employed successfully to reflect the chemical weathering intensity in various sediments (e.g. Zhao *et al.* 2005). Higher (lower) illite/chlorite ratio would suggest a higher (lower) chemical weathering intensity (Zhao *et al.* 2005). The illite/chlorite ratios from the Xiantai fluvio-lacustrine sediments show an up-section decreasing trend (Fig. 9b), suggesting a long-term decreasing trend in chemical weathering intensity in the Nihewan Basin over the past ∼2 Myr, that is, approximately from the onset of the Olduvai subchron.

Furthermore, the illite and chlorite contents also show a general up-section increasing trend (Figs 9c and d), which is consistent with the long-term decreasing trend in chemical weathering intensity in this region. Importantly, the *AH*-ratio changes in tune with chlorite content (Fig. 9e**)**, and shows a positive correlation to chlorite content (Fig. 8d) and a generally negative correlation to illite/chlorite (Fig. 8f), supporting that chlorite is the main factor giving rise to increased χ during heating. It should be noted that the *AH*-ratio changes by over two orders of magnitude, while the chlorite content changes only by a factor of below 3 (Fig. 8d). This suggests that a minute amount of altered chlorite would induce a large χ increase because the newly formed SP ferrimagnetic minerals have significantly high χ. In line with the long-term decreasing trend in chemical weathering intensity suggested by long-term changes in illite/chlorite ratio and illite and chlorite content, the *AH*-ratio changes display an up-section increasing trend as well (Fig. 9e). The decrease in chemical weathering intensity is able to decrease the *in situ* pedogenic formation of ferrimagnetic materials in the source areas, which may partially explain the long-term up-section decreasing trend in room-temperature χ of the unheated samples (Fig. 9a). The Nihewan Basin is dominated by an arid/semiarid continental climate that is at present characterized by moderately high temperatures and short periods of limited rainfall in summer. Therefore, the long-term decreasing trend in chemical weathering

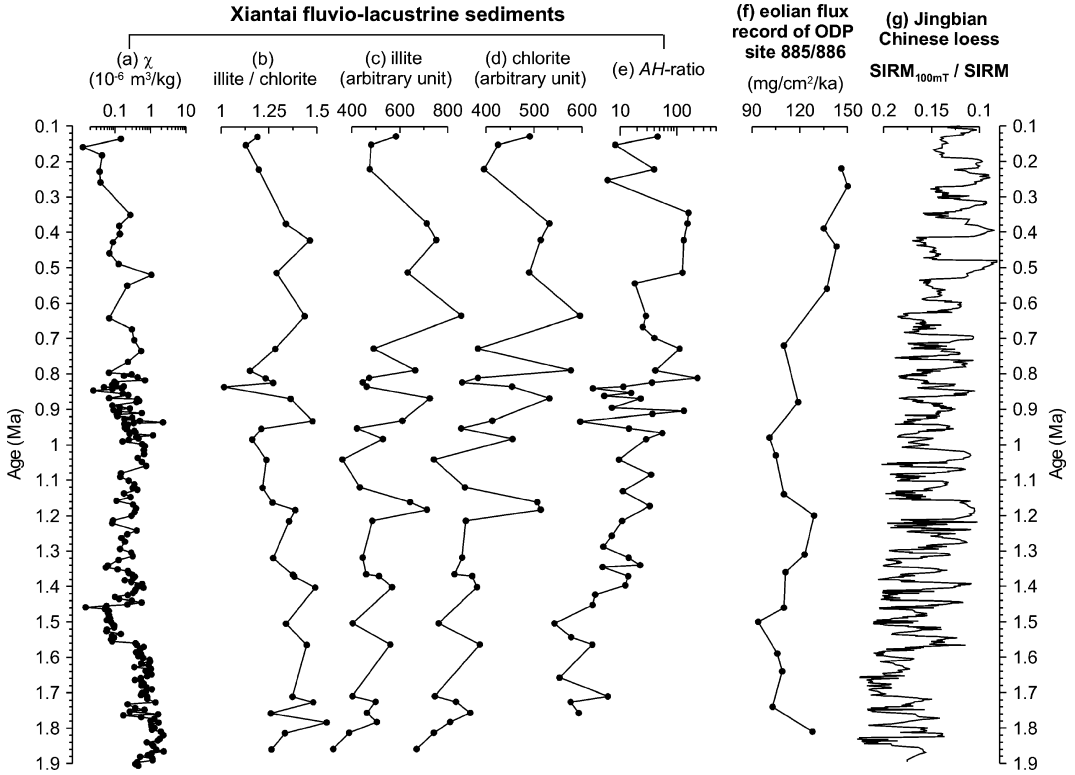

Figure 9. (a) magnetic susceptibility, (b) illite/chlorite ratios, (c) illite content, (d) chlorite content and (e) *AH*-ratio profile of the Xiantai section. (f) Mass accumulation rate of aeolian dust at ODP Site 885/886 (Rea *et al.* 1998). (g) $SIRM_{100mT}$/SIRM ratio from the Jingbian Chinese loess (SIRM is the saturation isothermal remanent magnetization, and $SIRM_{100mT}$ represents the residual SIRM after 100 mT alternating field demagnetization) (Deng *et al.* 2006b).

intensity inferred from the mineral-magnetic measurements (*AH*-ratio) and clay mineralogical parameters (illite/chlorite, illite and chlorite content) may imply a long-term increasing trend in aridification and cooling in the Nihewan Basin during the Pleistocene.

This intensified aridification and cooling in the Nihewan Basin during the Pleistocene inferred from the chemical weathering intensity is supported by the palynological record of this fluvio-lacustrine sequence at the Dadaopo section (Fig. 1b), ∼2 km west of the Xiantai section. This section is parallel to the adjacent Xiaodukou, Haojiatai and Taiergou sections, which has recorded a continuous magnetostratigraphy from the post-Olduvai Matuyama chron to the late Brunhes chron (Wang *et al.* 2004; Zhu *et al.* 2004; Li *et al.* 2008). The palynological record obtained from the Dadaopo section shows vegetation shifts from typical subtropical species, via a well-developed forest vegetation, to grasses and herbs (Yuan *et al.* 1996).

As suggested by the combined evidence, the intensified aridification and cooling in the Nihewan Basin during the Pleistocene is clearly documented, which is consistent with the Asian aridity recorded in the loess/palaeosol sequences of the Chinese Loess Plateau. The Nihewan Basin, located at the northeast margin of Loess Plateau (Fig. 1a), is suggested to show very similar climatic variations with the plateau under the influence of the East Asian monsoon. On the Chinese Loess Plateau, the intensified drying and cooling climate along with an increase (decrease) in winter (summer) monsoon intensity during Quaternary has been well suggested by various proxies (Kalm *et al.* 1996; An *et al.* 2001; Deng *et al.* 2005, 2006b). For example, the long-term decrease in the mineral magnetic proxies $SIRM_{100mT}$/SIRM (SIRM is the saturation isothermal remanent magnetization, and $SIRM_{100mT}$ represents the residual SIRM after 100 mT alternating field demagnetization) from the Jingbian Chinese loess-palaeosol sequence (Fig. 9g after Deng *et al.* 2006b), located at the northern extremity of the Chinese Loess Plateau (Fig. 1a), signals a long-term decreasing trend in the relative contribution of hematite in this sequence, which results from a long-term decrease in chemical weathering due to long-term increasing aridification and cooling in both the dust source areas and the Loess Plateau region (Deng *et al.* 2006b). In addition, this intensified Asian aridification and cooling is also supported by a decreasing trend in χ and an increasing trend in the coarse grain size fraction and Al flux (An *et al.* 2001), an increasing trend in the content of illite and chlorite (Kalm *et al.* 1996) and decreasing trends in the CIA (chemical index of alteration), Na/K, Rb/Sr, $^{87}Sr/^{86}Sr$ of the sediments from the Chinese Loess plateau (Chen *et al.* 2001). Furthermore, the development of this Asian aridification and cooling is also well recorded in marine sediments accumulated in the North Pacific Ocean (e.g. Rea *et al.* 1998), keeping in mind that these sediments formed in entirely different environments. During the Quaternary, for example, there is an increase in mass accumulation rate of aeolian dust in the North Pacific marine sediment at Ocean Drilling Program (ODP) Site 885/886 (Fig. 9f), representing a dessicating climate in Asia interior (Rea *et al.* 1998).

6 IMPLICATIONS AND CONCLUSIONS

In the above model, chemical weathering is considered as the main control on the observed variations in the thermally induced magnetic properties (i.e. *AH*-ratio) and clay mineralogy, and it provides a link between variation in magnetic properties and clay mineralogy and variation in climate. Although we cannot exclude other

possible magnetic phases and clay minerals that might have contributed to the increase in *AH*-ratio, the chlorite can be safely considered as, at least the main contributor, to the *AH*-ratio increase. The generally consistent variations in *AH*-ratio and clay mineralogical parameters (Fig. 9) suggest that *AH*-ratio can also signal the weathering extent as the clay mineralogical parameters. Compared to the measurements of clay mineralogical parameters, the measurement of thermally induced magnetic properties requires no chemical or physical pre-treatment on the samples and is cheaper, healthier, less time-consuming and simpler. Furthermore, despite that the increase in susceptibility after heating has been commonly interpreted to result from annealing of iron-containing clay minerals (e.g. Florindo *et al.* 1999), evidence was previously unavailable. Coupled with XRD spectra measurement, the present study shows that unstable iron-containing clay minerals such as chlorite are the main contributor to the increase in susceptibility during heating, and these iron-containing clay minerals are usually prone to weathering in the nature environment. The present investigation also documents that the thermally induced magnetic properties such as the *AH*-ratio may contain palaeclimatic information.

The desertification in the Asian interior, which has commenced at least 22 Ma (Guo *et al.* 2002), is a very important climate change in the late Cenozoic and is closely linked to the Tibetan uplift and cooling of the Northern Hemisphere (Rea *et al.* 1998). Due to this intensified Asian aridification and cooling, the deserts in northern China stepwise expanded and significant thick loess accumulated in northwestern China during the Quaternary (Ding *et al.* 2005). Meanwhile, the intensity of chemical weathering decreased in vast areas of China, including the Nihewan Basin. Up to now, the long-term reconstruction of Asian aridification is mainly based upon the terrestrial Chinese loess-palaesol and Pacific Ocean sediments (Rea *et al.* 1998; Guo *et al.* 2002; Ding *et al.* 2005; Deng *et al.* 2006b).

The present study suggests that the Nihewan fluvio-lacustrine sequence recorded this long-term palaeclimatic evolution as well, which can be well recognized by mineral-magnetic studies. The rapid and affordable mineral-magnetic investigation could provide a higher resolution climatic record than geochemical analyses or pollen analyses. Because the present mineral-magnetic and clay mineralogical investigation is mainly carried on selected typical samples, here it is hard to investigate the effects of glacial/interglacial oscillations on the long-term propensity of mineral-magnetic and clay mineralogical parameters. Further high-resolution and detailed mineral-magnetic studies on the Nihewan fluvio-lacustrine sequence may provide us with more detailed knowledge on the climatic evolution in North China.

There was a prominent early human flourishing in the Nihewan Basin in the Old World, in which most of the hominin or palaelithic sites in China spanning from 1.66 to 0.78 Ma were found (see reviews by Zhu *et al.* 2007). During this period, the environment in North China, including the Nihewan Basin, changed significantly: the intensified aridification and cooling, the interglacial/glacial oscillations, the replacement of forest vegetation by grasses and herbs and more variable climate during and after the mid-Pleistocene climate transition. Under those increasingly hostile and variable climatic conditions, the early humans had lived at least about 0.9 Myr in this high northern latitude area (around 40°N) in East Asia, showing high adaptability to the climatic variations (Zhu *et al.* 2004; Deng *et al.* 2006a, 2007). Early humans might have further expanded to north-central China during the early Pleistocene under the increasingly variable climate.

In summary, here a systemic rock magnetic and clay mineralogical investigation is carried on the Xiantai fluvio-lacustrine sequence. Released iron from decomposing chlorite induces formation of new fine-grained ferrimagnetic minerals during thermal treatment up to 700 °C, leading to a significant increase in susceptibility. Thus, the change in susceptibility of the Nihewan sedimentary sequence after annealing at 700 °C signals the variation of its chlorite content, which, in turn, serves as a useful measure of palaeclimatic change in this area. A long-term increase in aridification and cooling in the Nihewan Basin during the Pleistocene is well suggested by the magnetoclimatological proxy *AH*-ratio and by the clay mineralogical proxies, such as the illite/chlorite ratio, the chlorite content and illite content, from the Xiantai fluvio-lacustrine sequence. This long-term palaeclimatic variation agrees with the Asian aridity suggested by a series of palaeclimatic records from the Chinese loess-palaesol sequences and by the aeolian flux record from the ODP Site 885/886 (e.g. Kalm *et al.* 1996; Rea *et al.* 1998; An *et al.* 2001; Chen *et al.* 2001; Deng *et al.* 2006b). Furthermore, the palaeenvironmental changes suggested by our present investigation provide the general setting for early human evolution in high northern latitude in East Asia.

ACKNOWLEDGMENTS

We are grateful to the Editor, Prof. Erwin Appel, to the GJI reviewers Friedrich Heller and Leonardo Sagnotti and an anonymous reviewer for their insightful comments to improve the manuscript. We thank Profs. Qingsong Liu and Jimin Sun for their insightful suggestions. We also thank Hongqiang Wang, Rui Zhang and Liao Chang for their field assistance. All the magnetic measurements were made in the Palaemagnetism Geochronology Laboratory (SKL-LE), Institute of Geology and Geophysics, Chinese Academy of Sciences. The XRD measurement was carried out in the Earth's Material Composition and Property Analysis System of this institute. Financial assistance was provided by the Ministry of Science and Technology of China (grant 2007FY110200), the National Natural Science Foundation of China (grants 40221402 and 40325011) and the Chinese Academy of Sciences.

REFERENCES

An, Z.S., Kutzbach, J.E., Prell, W.L. & Porter, S.C., 2001. Evolution of Asian monsoons and phased uplift of the Himalayan-Tibetan plateau since Late Miocene times, *Nature,* **411,** 62–66.

Ao, H., 2008. Rock magnetic properties of the fluvio-lacustrine sediments from the Dachangliang section in the Nihewan Basin, northern China (in Chinese with English abstract), *Chin. J. Geophys.,* **51,** 1029–1039.

Ao, H., Liu, C.C. & Deng, C.L., 2007. Wasp-waisted hysteresis loops from the Dachangliang fluvio-lacustrine sequence in the Nihewan Basin, North China and its paleoclimatic significance (in Chinese with English abstract), *Quat. Sci.,* **27,** 1072–1080.

Berggren, W.A., Kent, D.V., Swisher 3rd, C.C. & Aubry, M.P., 1995. A revised Cenozoic geochronology and chronostratigraphy in time scales and global stratigraphic correlations: a unified temporal framework for an historical geology, in *Geochronology, Timescales, and Stratigraphic Correlation,* Spec. Publ. No. 54, pp. 129–212, eds Berggren, W.A., Kent, D.V., Aubry, M.P. & Hardenbol, J., Society of Economic Paleontologists and Mineralogists, Tulsa, OK.

Chen, J., An, Z.S., Liu, L.W., Ji, J.F., Yang, J.D. & Chen, Y., 2001. Variations in chemical compositions of the aeolian dust in Chinese Loess Plateau over the past 2.5 Ma and chemical weathering in the Asian inland, *Sci. China (Ser. D),* **44,** 403–413.

Coey, J.M.D., 1988. *Magnetic Properties of Soil Iron Oxides and Clay minerals,* Reidel Publishing, Dordrecht.

Day, R., Fuller, M. & Schmidt, V., 1977. Hysteresis properties of titanomagnetites: grain size and composition dependence, *Phys. Earth planet. Inter.,* **13,** 260–267.

de Boer, C.B. & Dekkers, M.J., 2001. Unusual thermomagnetic behaviour of haematites: neoformation of a highly magnetic spinel phase on heating in air, *Geophys. J. Int.,* **144,** 481–494

Deng, C.L., Vidic, N.J., Verosub, K.L., Singer, M.J., Liu, Q.S., Shaw, J. & Zhu, R.X., 2005. Mineral magnetic variation of the Jiaodao Chinese loess/paleosol sequence and its bearing on long-term climatic variability, *J. geophys. Res.,* **110,** B03103, doi:10.1029/2004JB003451.

Deng, C.L., Wei, Q., Zhu, R.X., Wang, H.Q., Zhang, R., Ao, H., Chang, L. & Pan, Y.X., 2006a. Magnetostratigraphic age of the Xiantai Paleolithic site in the Nihewan Basin and implications for early human colonization of Northeast Asia, *Earth planet. Sci. Lett.,* **244,** 336–348.

Deng, C.L., Shaw, J., Liu, Q.S., Pan, Y.X. & Zhu, R.X., 2006b. Mineral magnetic variation of the Jingbian loess/paleosol sequence in the northern Loess Plateau of China: implications for Quaternary development of Asian aridification and cooling, *Earth planet. Sci. Lett.,* **241,** 248–259.

Deng, C.L., Xie, F., Liu, C.C., Ao, H., Pan, Y.X. & Zhu, R.X., 2007. Magnetochronology of the Feiliang Paleolithic site in the Nihewan Basin and implications for early human adaptability to high northern latitudes in East Asia, *Geophys. Res. Lett.,* **34,** L14301, doi:10.1029/2007GL030335.

Deng, C.L., Zhu, R.X., Zhang, R., Ao, H. & Pan, Y.X., 2008. Timing of the Nihewan Formation and faunas, *Quat. Res.,* **69,** 77–90.

Ding, Z.L., Derbyshire, E., Yang, S.L., Yu, Z.W., Xiong, S.F. & Liu, T.S., 2002. Stacked 2.6-Ma grain size record from the Chinese loess based on five sections and correlation with the deep-sea δ^{18}O record, *Paleoceanography,* **17,** 1033, doi: 10.1029/2001PA000725.

Ding, Z.L., Derbyshire, E., Yang, S.L., Sun, J.M. & Liu, T.S., 2005. Stepwise expansion of desert environment across northern China in the past 3.5 Ma and implications for monsoon evolution, *Earth planet. Sci. Lett.,* **237,** 45–55.

Dunlop, D.J., 2002a. Theory and application of the Day plot (M_{rs}/M_s versus H_{cr}/H_c) 1. Theoretical curves and tests using titanomagnetite data, *J. geophys. Res.,* **107,** 2076, doi:10.1029/2001JB000486.

Dunlop, D.J., 2002b. Theory and application of the Day plot (M_{rs}/M_s versus H_{cr}/H_c), 2: application to data for rocks, sediments, and soils, *J. geophys. Res.,* **107,** 2057, doi:10.1029/2001JB000487.

Dunlop, D.J. & Özdemir, Ö., 1997. *Rock Magnetism: Fundamentals and Frontiers,* Cambridge University Press, Cambridge, UK.

Evans, M.E. & Heller, F., 2003. *Environmental Magnetism: Principles and Applications of Enviromagnetics,* Academic Press, Oxford.

Florindo, F., Zhu, R.X., Guo, B., Yue, L.P., Pan, Y.X. & Speranza, F., 1999. Magnetic proxy climate results from the Duanjiapo loess section, southernmost extremity of the Chinese loess plateau, *J. geophys. Res.,* **104,** 645–659.

Guo, Z.T. *et al*. 2002. Onset of Asian desertification by 22 Myr ago inferred from loess deposits in China, *Nature,* **416,** 159–163.

Heller, F. & Evans, M.E., 1995. Loess Magnetism, *Rev. Geophys.,* **33,** 211–240.

Hilton, J., 1987. A simple model for the interpretation of magnetic records in lacustrine and ocean sediments, *Quat. Res.,* **27,** 160–166.

Hirt, A.M., Banin, A. & Gehring, A.U., 1993. Thermal generation of ferromagnetic minerals from iron-enriched smectites, *Geophys. J. Int.,* **115,** 1161–1168.

Hu, S.Y., Deng, C.L., Appel, E. & Verosub, K.L., 2002. Environmental magnetic studies of lacustrine sediments, *Chin. Sci. Bull.,* **47,** 613–616.

Ji, J.F., Chen, J., Liu, L.W., and Lu, H.Y., 1999. Chemical weathering of chlorite and increase of susceptibility in Luochuan loess, *Prog. Nat. Sci.,* **9,** 619–623.

Kalm, V.E., Rutter, N.W. & Rokosh, C.D., 1996. Clay minerals and their paleoenvironmental interpretation in the Baoji loess section, Southern Loess Plateau, China, *Catena,* **27,** 49–61.

Li, H.M., Yang, X.Q., Heller, F., & Li, H.T., 2008. High resolution magnetostratigraphy and deposition cycles in the Nihewan Basin (North China) and their significance for stone artifact dating, *Quat. Res.,* **69,** 250–262.

Liu, Q.S., Deng, C.L., Yu, Y.J., Torrent, J., Jackson, M.J., Banerjee, S.K. & Zhu, R.X., 2005. Temperature dependence of magnetic susceptibility in an argon environment: implications for pedogenesis of Chinese loess/palaeosols, *Geophys. J. Int.,* **161,** 102–112.

Liu Q.S., Deng, C.L., Torrent, J., Zhu, R.X., 2007. Review of recent developments in mineral magnetism of the Chinese loess, *Quat. Sci. Rev.,* **26,** 368–385.

Løvlie, R., Su, P., Fan, X.Z., Zhao, Z.J. & Liu, C., 2001. A revised paleomagnetic age of the Nihewan Group at the Xujiayao Palaeolithic Site, China, *Quat. Sci. Rev.,* **20,** 1341–1353.

Moskowitz, B.M., Frankel, R.B. & Bazylinski, D.A., 1993. Rock magnetic criteria for the detection of biogenic magnetite, *Earth planet. Sci. Lett.,* **120,** 283–300.

Oches, E.C. & Banerjee, S.K., 1996. Rock-magnetic proxies of climate change from loess-paleosol sediments of the Czech Republic, *Stud. Geophys. Geodaet.,* **40,** 287–300.

Passier, H.F. & Dekkers, M.J., 2002. Iron oxide formation in the active oxidation front above sapropel S1 in the eastern Mediterranean Sea as derived from low-temperature magnetism, *Geophys. J. Int.,* **150,** 230–240.

Pei, S.W., 2002. The Paleolithic site at Dachangliang in the Nihewan Basin, north China (in Chinese with English abstract), *Acta Anthropol. Sin.,* **21,** 116–125.

Pike, C.R., Roberts, A.P. & Verosub, K.L., 2001. First-order reversal curve diagrams and thermal relaxation effects in magnetic particles, *Geophys. J. Int.,* **145,** 721–730.

Proust, D., Eymery, J.P. & Beaufort, D., 1986. Supergene vermiculitization of a magnesian chlorite: iron and magnesium removal processes, *Clays Clay Mineral.,* **34,** 572–580.

Qiu, Z.X., 2000. Nihewan fauna and Q/N boundary in China (in Chinese with English abstract), *Quat. Sci.,* **20,** 142–154.

Rea, D.K., Snoeckx, H. & Joseph, L.H., 1998. Late Cenozoic eolian deposition in the North Pacific: Asian drying, Tibetan uplift, and cooling of the northern hemisphere, *Paleoceanography,* **13,** 215–224.

Righi, D., Velde, B. & Meunier, A., 1995. Clay stability in clay-Dominated soil systems, *Clay Mineral.,* **30,** 45–54.

Roberts, A.P., 1995. Magnetic properties of sedimentary Greigite (Fe_3S_4), *Earth planet. Sci. Lett.,* **134,** 227–236.

Roberts, A.P., Cui, Y.L. & Verosub, K.L., 1995. Wasp-waisted hysteresis loops: mineral magnetic characteristics and discrimination of components in mixed magnetic systems, *J. geophys. Res.,* **100,** 17 909–17 924.

Roberts, A.P., Pike, C.R. & Verosub, K.L.,2000. First-order reversal curve diagrams: a new tool for characterizing the magnetic properties of natural samples, *J. geophys. Res.,* **105,** 28 461–28 475.

Rowan, C.J. & Roberts, A.P., 2006. Magnetite dissolution, diachronous greigite formation, and secondary magnetizations from pyrite oxidation: unravelling complex magnetizations in Neogene marine sediments from New Zealand, *Earth planet. Sci. Lett.,* **241,** 119–137.

Sagnotti, L., Florindo, F., Verosub, K.L., Wilson, G.S. & Roberts, A.P., 1998. Environmental magnetic record of Antarctic palaeoclimate from Eocene/Oligocene glaciomarine sediments, Victoria Land Basin, *Geophys. J. Int.,* **134,** 653–662.

Singer, B.S., Hoffman, K.A., Chauvin, A., Coe, R.S. & Pringle, M.S., 1999. Dating transitionally magnetized lavas of the late Matuyama Chron: toward a new 40Ar/39Ar timescale of reversals and events, *J. geophys. Res.,* **104,** 679–693.

Singer, B.S., Relle, M.K., Hoffman, K.A., Battle, A., Laj, C., Guillou, H. & Carracedo, J.C., 2002. Ar/Ar ages from transitionally magnetized lavas on La Palma, Canary Islands, and the geomagnetic instability timescale, *J. geophys. Res.,* **107,** 2307, doi:10.1029/2001JB001613.

Teilhard de Chardin, P. & Piveteau, J., 1930. Les mammiferes fossils de Nihowan (Chine), *Ann. Paléontol.,* **19,** 1–154.

Verosub, K.L. & Roberts, A.P., 1995. Environmental magnetism: past, present, and future, *J. geophys. Res.,* **100,** 2175–2192.

Wan, S.M., Li, A.C., Clift, P.D. & Jiang, H.Y., 2006. Development of the East Asian summer monsoon: evidence from the sediment record in the South China Sea since 8.5 Ma, *Palaeogeogr. Palaeoclimatol. Palaeoecol.,* **241,** 139–159.

Wan, S.M., Li, A.C., Clift, P.D. & Stuut, J.B.W., 2007. Development of the East Asian monsoon: mineralogical and sedimentologic records in

the northern South China Sea since 20 Ma, *Palaeogeogr. Palaeoclimatol. Palaeoecol.,* **254,** 561–582.

Wang, H.Q., 2007. Magnetic properties of lacustrine sediments at the Donggutuo section in the Nihewan basin and their environmental significance (in Chinese with English abstract), *Quat. Sci.,* **27,** 1081–1091.

Wang, H.Q., Deng, C.L., Zhu, R.X., Wei, Q., Hou, Y.M. & Boëda, E., 2005. Magnetostratigraphic dating of the Donggutuo and Maliang Paleolithic sites in the Nihewan Basin, North China, *Quat. Res.,* **64,** 1–11.

Wang, H.Q., Deng, C.L., Zhu, R.X. & Xie, F., 2006. Paleomagnetic dating of the Cenjiawan Paleolithic site in the Nihewan Basin, northern China, *Sci. China (Ser. D),* **49,** 295–303.

Wang, X.S., Løvlie, R. & Su, P., 2002. Rock magnetic properties of Nihewan sediments at Xujiayao, *Sci. China (Ser. D),* **32,** 271–278.

Wang, X.S., Yang, Z.Y., Lovlie, R. & Min, L.R., 2004. High-resolution magnetic stratigraphy of fluvio-lacustrine succession in the Nihewan Basin, China, *Quat. Sci. Rev.,* **23,** 1187–1198.

Wang, X.S., Løvlie, R., Su, P. & Fan, X.Z., 2008. Magnetic signature of environmental change reflected by Pleistocene lacustrine sediments from the Nihewan Basin, North China, *Palaeogeogr. Palaeoclimatol. Palaeoecol.,* **260,** 452–462.

Yuan, B.Y., Zhu, R.X., Tian, W.L., Cui, J.X., R.Q., L., Wang, Q. & Yan, F.H., 1996. The age, subdivision and correlation of Nihean Group (in Chinese), *Sci. China (Ser. D),* **26,** 67–76.

Zhao, L., Ji, J.F., Chen, J., Liu, L.W., Chen, Y. & Balsam, W., 2005. Variations of illite/chlorite ratio in Chinese loess sections during the last glacial and interglacial cycle: implications for monsoon reconstruction, *Geophys. Res. Lett.,* **32,** L20718, dio:10.1029/2005GL024145.

Zhu, R.X. *et al.*, 2001. Earliest presence of humans in northeast Asia, *Nature,* **413,** 413–417.

Zhu, R.X., An, Z.S., Potts, R. & Hoffman, K.A., 2003. Magnetostratigraphic dating of early humans in China, *Earth-Sci. Rev.,* **61,** 341–359.

Zhu, R.X. *et al.*, 2004. New evidence on the earliest human presence at high northern latitudes in northeast Asia, *Nature,* **431,** 559–562.

Zhu, R.X., Deng, C.L. & Pan, Y.X., 2007. Magnetochronology of the fluvio-lacustrine sequences in theNihewan basin and its implications for early human colonization of Northeast Asia (in Chinese with English abstract), *Quat. Sci.,* **27,** 922–944.